Molecular Vision 2020; 26:48-62 <http://www.molvis.org/molvis/v26/48>
Received 5 September 2019 | Accepted 21 February 2020 | Published 24 February 2020

A method for gene knockdown in the retina using a lipid-based carrier

Joshua A. Chu-Tan,[1,2] Nilisha Fernando,[1] Riemke Aggio-Bruce,[1] Adrian V. Cioanca,[1] Krisztina Valter,[1,2] Nektaria Andronikou,[1,3] Xavier deMollerat du Jeu,[1,3] Matt Rutar,[4] Jan Provis,[1,2] Riccardo Natoli[1,2]

[1]The John Curtin School of Medical Research, The Australian National University, Acton, ACT, Australia; [2]The Australian National University Medical School, Acton, Australia; [3]Thermo Fisher Scientific, Carlsbad, CA; [4]School of Biomedical Sciences, The University of Melbourne, Kenneth Myer Building, Melbourne, Australia

Purpose: The use of small non-coding nucleic acids, such as siRNA and miRNA, has allowed for a deeper understanding of gene functions, as well as for development of gene therapies for complex neurodegenerative diseases, including retinal degeneration. For effective delivery into the eye and transfection of the retina, suitable transfection methods are required. We investigated the use of a lipid-based transfection agent, Invivofectamine® 3.0 (Thermo Fisher Scientific), as a potential method for delivery of nucleic acids to the retina.

Methods: Rodents were injected intravitreally with formulations of Invivofectamine 3.0 containing scrambled, *Gapdh, Il-1β*, and *C3* siRNAs, or sterile PBS (control) using a modified protocol for encapsulation of nucleic acids. TdT-mediated dUTP nick-end labeling (TUNEL) and IBA1 immunohistochemistry was used to determine histological cell death and inflammation. qPCR were used to determine the stress and inflammatory profile of the retina. Electroretinography (ERG) and optical coherence tomography (OCT) were employed as clinical indicators of retinal health.

Results: We showed that macrophage recruitment, retinal stress, and photoreceptor cell death in animals receiving Invivofectamine 3.0 were comparable to those in negative controls. Following delivery of Invivofectamine 3.0 alone, no statistically significant changes in expression were found in a suite of inflammatory and stress genes, and ERG and OCT analyses revealed no changes in retinal function or morphology. Injections with siRNAs for proinflammatory genes (*C3* and *Il-1β*) and *Gapdh*, in combination with Invivofectamine 3.0, resulted in statistically significant targeted gene knockdown in the retina for up to 4 days following injection. Using a fluorescent Block-It siRNA, transfection was visualized throughout the neural retina with evidence of transfection observed in cells of the ganglion cell layer, inner nuclear layer, and outer nuclear layer.

Conclusions: This work supports the use of Invivofectamine 3.0 as a transfection agent for effective delivery of nucleic acids to the retina for gene function studies and as potential therapeutics.

Delivery of small nucleic acids as a gene therapy has been intensely investigated for the treatment of neurodegenerative diseases, including retinal degenerations [1-8]. The eye is the ideal structure for developing and testing translational gene therapies for neurodegeneration due to the small size and enclosed structure, immune privilege, and easy accessibility of the eye and the availability of animal models for retinal diseases [9,10].

However, delivery of drugs to the retina located in the posterior part of the eye has historically been challenging [11]. Intravitreal delivery of drugs is a commonly used technique that requires injection into the vitreous body of the eye. However, frequent administration of intravitreal injections can lead to several complications, including retinal detachment, endophthalmitis, and increased intraocular pressure [11,12], an issue that may be bypassed with the development of new topical ocular formulations with the ability to reach the retina [13]. In addition to the complexities of retinal physiology that deem delivery to the tissue challenging, the stability and actual transfection efficiency of small nucleic acids injected into the eye have to be considered [14].

For a gene therapy to be effective, an efficient vector or carrier is required. Several key aspects are crucial for effective gene therapy vectors: enhancing gene transfer efficiency, cell specificity, safety, and long-term expression [15,16]. In the past decade, there have been significant efforts in improving the delivery of small nucleic acids directed toward finding safe and efficient gene therapy reagents and vehicles. They can be split into two major groups: viral vectors and non-viral vectors.

Viral vectors include lentiviruses and retroviruses, but the one with the most success in terms of intraocular delivery is the use of adenoassociated viruses (AAVs) [17–19]. However, there are limitations regarding the consistent use

Correspondence to: Riccardo Natoli, Clear Vision Research Laboratory, Eccles Institute of Neuroscience, John Curtin School of Medical Research, College of Health and Medicine, The Australian National University, Acton, ACT 2601, Australia; Phone: +61 2 612 58559; email: riccardo.natoli@anu.edu.au

of AAVs within the eye, specifically their tendency to cause inflammatory responses at high doses, limiting their ability to be repeatedly injected [20-25].

Lipid-based transfection agents have been explored as a potentially safer alternative to viral vectors due to the ease of their production and low toxicity (reviewed in [10]). Many efforts in the past decade have gone into improving transfection efficiency of lipid-based formulations with limited toxicity [26]. Lipid-based nanosystems, including solid lipid nanoparticles and liposomes, have been shown to be efficient carriers of siRNA to the retina to manage retinal diseases [14]. Invivofectamine 3.0 (Thermo Fisher Scientific, Waltham, MA) was developed as a lipid-based carrier for in vivo work to enhance delivery to the target tissue while minimizing unwanted cytotoxicity within the tissue. Previous studies have demonstrated the use of Invivofectamine as a mode of delivery to the retina [27,28], where the difficulties of reduced transfection efficiency due to the inner limiting membrane (ILM) were overcome [29,30].

In this study, we demonstrate the efficacy of Invivofectamine 3.0 as a carrier for siRNA into the retina. The results indicate that the use of Invivofectamine 3.0 lipid-based transfection is a quick, low-toxicity, and efficient method for retinal transfection of small nucleic acids with minimal to no toxicity or negative effects on retinal function, inflammation, or cell death. This is a simple method for modulating and controlling dysregulated gene expression using siRNA in rodent animal models.

METHODS

Animals: All animal procedures were conducted in accordance with the Association for Research in Vision and Ophthalmology (ARVO) Statement for the Use of Animals in Ophthalmic and Vision Research, as well as the Australian National University (ANU) Animal Experimentation Ethics Committee (Protocol Number: A2014/56, A2017/41). Adult albino Sprague-Dawley (SD) rats age between 90 and 120 days and C57BL/6J mice age between 60 and 90 days were used for all experiments. The animals were born and raised in a 12 h:12 h light-dark cycle in dim light conditions (5 lux). Atropine sulfate 1% w/v eye drops (Bausch and Lomb, Sydney, Australia) were used to dilate pupils during photo-oxidative damage in mice and before intravitreal injections. Ketamine (100 mg/kg; Troy Laboratories, Glendenning, Australia) and xylazil (12 mg/kg; Troy Laboratories) were used to anesthetize animals before the intravitreal injections, electroretinography (ERG), and optical coherence tomography (OCT) were performed.

Preparation of encapsulated small nucleic acids with Invivofectamine 3.0: The procedure for the preparation of siRNAs is outlined in Figure 1. SiRNAs were encapsulated using Invivofectamine 3.0, a cationic liposome-based formulation according to the manufacturer's instructions (Thermo Fisher Scientific) with some modifications. The SiRNAs used in this study are listed in Table 1. The following equates to the protocol used for siRNA with a molecular weight of 13,000 g/mol:

Equal volumes of siRNA (diluted to 2.4 µg/µl in nuclease-free water) and complexation buffer were mixed. The siRNA:complexation buffer solution was then mixed in a 1:1 ratio with the Invivofectamine 3.0 formulation warmed to room temperature. The mixture was then incubated for 30 min at 50 °C. Following the incubation step, the mixture was diluted 15-fold in 0.1 M sterile, endotoxin-free UltraPure PBS (Thermo Fisher Scientific, Waltham, MA). Diafiltration was conducted using an Amicon Ultra-4 Centrifugal Filter Unit (Merck Millipore, Burlington, MA) to purify the siRNA:Invivofectamine 3.0 complexes. The siRNA:Invivofectamine 3.0 complex was added to the filter column and spun at 4,000 ×*g* for approximately 1 h to purify and concentrate the solution to 2 µg/µl. The concentrated complex was then diluted with sterile 0.1 M PBS, so that each siRNA complex was encapsulated at a final concentration of 0.33 µg/µl in sterile PBS unless stated otherwise. The concentrations of siRNA used were based on previously published studies [27,28].

Preparation of encapsulated small nucleic acids with in vivo-jetPEI®: Silencer™ FAM-labeled GAPDH siRNA (Thermo Fisher Scientific) was reconstituted in nuclease-free water at a stock concentration of 4 µg/µl and diluted in 10% glucose solution in nuclease-free water. The *in vivo*-jetPEI® (Polyplus transfection, Illkirch, France) transfection reagent was prepared in 10% glucose solution in nuclease-free water and used at an nitrogen/nucleic acid phosphate (N/P) ratio of 7 (0.14 µl of transfection reagent per 1 µg of GAPDH siRNA). Equal volumes of the siRNA solution and the *in vivo*-jetPEI® solution were mixed and incubated at room temperature for 15 min to achieve complexation. The maximum concentration of nucleic acid that could be encapsulated was 0.5 µg of *Gapdh* siRNA which was delivered intravitreally at a final glucose concentration of 5%.

Intravitreal injections: Intravitreal injections were performed as outlined schematically in Figure 1 and Figure 2. Animals were anesthetized using an intraperitoneal injection of ketamine (100 mg/kg) and xylazil (12 mg/kg). A pupil dilator (tropicamide 0.5% w/v eye drops; Bausch and Lomb) was administered to the ocular surface of each eye (Figure 2A).

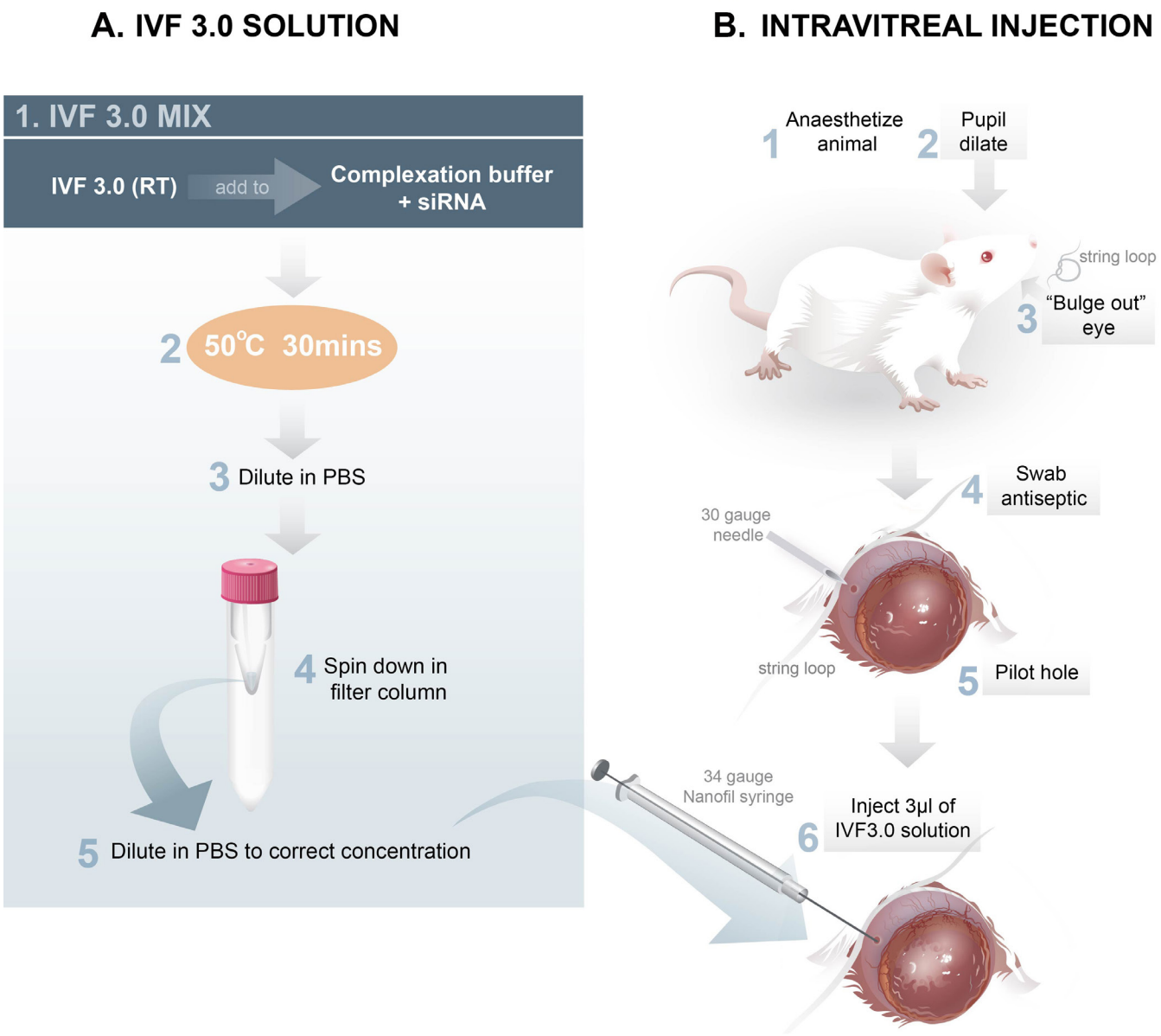

Figure 1. Schematic of Invivofectamine 3.0 preparation and intravitreal injections. **A**: Invivofectamine 3.0 was added to a mixture of complexation buffer and siRNA of choice. This solution was incubated for 30 min at 50 °C. The solution was diluted in PBS and then spun down in a filter column to the correct concentration, which then was ready for injection. **B**: The animals were anesthetized and their pupils dilated with atropine sulfate. The eye was then drawn forward with a string loop. Betadine iodine was swabbed on the injection site before insertion of the pilot hole with a 30-gauge needle. The 34-gauge NanoFil syringe was then inserted and 3 µl (for rats) or 1 µl (for mice) of the solution injected. The injection process is described in more detail in Figure 2.

A string loop was tied around the eye to allow for easier access to the injection site (Figure 2B). The injection site was swabbed with 5% povidone iodine (Betadine, Mundipharma, Sydney, Australia) before the injection (Figure 2C). siRNA:Invivofectamine 3.0 complexes were injected intravitreally into the rodent eyes with the aid of a stereo microscope (M125; Leica Microsystems, Wetzlar, Germany). A 30-gauge needle was first used to make a punch incision, 0.5 mm posterior to the temporal limbus. A 10 µl NanoFil syringe with an attached 34 gauge NanoFil needle (World Precision Instruments, Sarasota, FL) was then inserted through the incision, angled toward the optic nerve (Figure 2D–F). Three microliters of the complex was injected into each rat eye at a concentration of 0.33 µg/µl, and 1 µl into each mouse eye at a concentration of 1 µg/µl (Figure 2G). The cloudiness of Invivofectamine 3.0 was visible through the animal eye

Table 1. siRNA complexes for intravitreal delivery.

siRNA complex	Company	Catalogue number
Gapdh **(Glyceraldehyde 3-phosphate dehydrogenase)**	Thermo Fisher Scientific	AM4650
Il-1β **(Interleukin-1β)**	Thermo Fisher Scientific	s127941
C3 **(Complement component C3)**	Thermo Fisher Scientific	s63165
Block-It Alexa Fluor Red	Thermo Fisher Scientific	14,750,100
Scrambled negative siRNA	Thermo Fisher Scientific	12,935,300

(Figure 2G,H). Animals were injected with positive siRNA (Table 1), negative siRNA, or Invivofectamine 3.0 only. Two additional controls were used: PBS only and needle-stick only (a punch incision was made, and the 34G needle was inserted and removed without injection). Post-injection, the injection site was swapped with Chlorsig (Alcon, Fort Worth, TX) followed by administration of GenTeal eye gel (0.3% hydroxypropyl methylcellulose and 0.22% carbomer 980, Aspen Pharmacare, KwaZulu-Natal, South Africa), which hydrated the cornea until full recovery. The animals were put back into dim-reared conditions for 1, 3, 5, and 7 days before tissue collection. For photo-oxidative damage (PD), animals recovered after anesthesia before being placed into PD. Tissue was collected at the end of the PD time period.

Photo-oxidative damage: To induce retinal stress, we implemented a PD paradigm. The adult SD rats were placed in transparent Perspex open-top cages under a light source (COLD F2, 2×36W, IHF, Thorn Lighting, Spennymoor, United Kingdom) at 1,000 lux for 24 h, with access to food and water ad libitum [31]. The C57BL/6J mice were housed in custom-made Perspex boxes coated with a reflective interior, and exposed to 100 K lux of natural white light-emitting diode (LED) for up to 7 days, with free access to food and water [32]. Each animal was administered pupil dilator eye drops (atropine sulfate 1% w/v, Bausch and Lomb, Rochester, MN) twice daily during PD.

Tissue collection and processing: The animals were singly euthanized with CO_2 gas inhalation in a sealed cage.The superior surface of the eye was marked before extraction for orientation purposes. Whole eyes were injected and immersion fixed with 4% paraformaldehyde for 4 h at 4 °C and then processed as described previously [33,34]. The eyes were sectioned in the parasagittal plane at a thickness of 16 µm and mounted on poly-L-lysine slides. Retinas were collected via a corneal incision for RNA extraction (further described in section “Quantitative real-time PCR”).

Measurement of retinal function using ERG: Full-field scotopic ERG was performed to assess the animals’ retinal function after intravitreal injections as described previously [32]. ERG was performed using an LED-based system (FS-250A Enhanced Ganzfeld, Photometric Solutions International, Huntingdale, Australia). Briefly, mice were dark-adapted overnight, anesthetized using an intraperitoneal injection of ketamine (100 mg/kg) and xylazil (12 mg/kg), and the pupils dilated with 1% w/v atropine sulfate (Bausch and Lomb). A single- or twin-flash paradigm over a stimulus intensity range of 6.3 log cd s m^{-2} (range −4.4 to 1.9 log cd s m^{-2}) was used to elicit mixed (rod and cone) or isolated cone responses, respectively. Measurements of the cone a-wave and b-wave responses were performed using Lab Chart 8 (AD Instruments, Dunedin, New Zealand).

Optical coherence tomography: Spectralis OCT (Heidelberg Engineering, Heidelberg, Germany) was used to determine changes in retinal morphology. OCT and fundus images of the retina were analyzed using ImageJ software (National Institutes of Health, Bethesda, MD) as previously described [28] at 1 and 7 days post-injection. Animals were anaesthetized and restrained on a custom-made platform attached to the OCT machine. A rodent contact lens was placed on the eye (polymethylmethacrylate [PMMA] lenses, radius of curvature of the central optic zone of 2.70 mm and diameter of 5.20 mm, Cantor + Nissel, Brackley, UK). Fundus and cross-sectional images were taken from 0 to 3 mm superior to the optic nerve. Retinal thickness and outer nuclear layer (ONL) depth were measured in two OCT transects per retina in the region of interest (1–2 mm superior to the optic nerve), which is the location of focal retinal damage in rodents in PD [32], with three points sampled across each image. The ONL thickness ratios were calculated as the ONL thickness relative to the distance between the outer limiting membrane (OLM) and the ILM. Fundus images of the area of interest (superior to the optic nerve) were taken to detect any retinal lesions.

TUNEL analysis of cell death: TdT-mediated dUTP nick-end labeling (TUNEL) was used to quantify photoreceptor cell death in retinal cryosections, using a previously published protocol [35] with an In Situ Cell Death Detection Kit (Roche Diagnostics, Risch-Rotkreuz, Switzerland). TUNEL positive cells were counted in the ONL along the full length of the retinal sections cut on the superoinferior plane including the optic disc. The final counts for each experimental group were the average of at least four biological replicates counted at comparable locations in the retina.

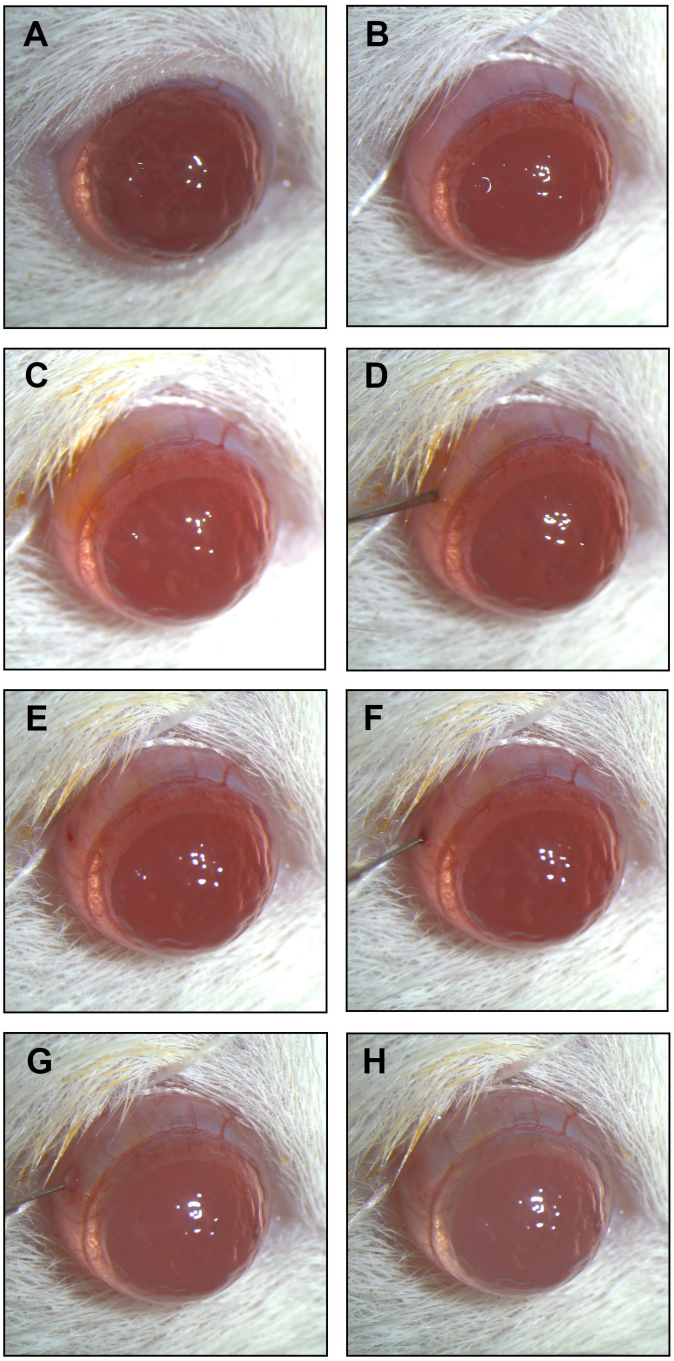

Figure 2. Images of intravitreal injection into the rat eye. **A**: Rat eye after administration of atropine sulfate for pupil dilation. **B**: A string loop was tied around the eye to "bulge out" the eye. **C**: Betadine iodine was swabbed on the surface of the sclera at the injection site. **D**: A pilot hole was made in the superotemporal region with a 30-gauge needle on the sclera behind the lens. **E**: The pilot hole is clearly seen on the sclera. **F**: A 34-gauge needle attached to a NanoFil syringe was used for injections and was inserted into the pilot hole at a similar angle. **G**: The cloudy Invivofectamine 3.0 solution was injected and should be visible through the lens. **H**: Chlorsig antibiotic was swabbed on the injection site with GenTeal eye gel applied to prevent dryness.

Immunohistochemistry: Immunohistochemistry was performed on retinal cryosections according to previously described protocols, with minor modifications [36]. IBA1 (1:500, Wako, Osaka, Japan) and GFAP (1:500, Dako, Glostrup, Denmark) were used as primary antibodies, which were later conjugated to Alexa-488 or Streptavidin-594 (Thermo Fisher Scientific) as secondary antibodies. Fluorescence in sections was captured in Z-stacked form, using a laser-scanning A1$^+$ confocal microscope. Images were captured using the same gain settings and processed using Photoshop CS6 software (Adobe Systems, San Jose, CA). Immunolabeled IBA1 positive mononuclear phagocytes (microglia and macrophages) were quantified across the full length of each section in the parasagittal plane (superoinferior), with the total count per retinal section including inner and outer retinal microglia and macrophages.

Optical densitometry: Optical densitometry was used to determine relative fluorescence intensity and transfection efficiency of fluorescent Block-It siRNA. All sections were measured in three different locations in the same retinal region (superior, 2–3 mm from the optic nerve due to the larger rat retina [31]). The measurements were taken from the whole retinal region from the ILM to the OLM. In addition, single layer measurements were taken from the ganglion cell layer (GCL), inner nuclear layer (INL), and ONL individually, in arbitrary fluorescence intensity units. All regions of interest were measured using the Nikon A1$^+$ confocal microscope.

Quantitative real-time PCR: Total RNA was extracted from the retinal samples in microscale according to the manufacturer's protocol (RNAqueous Total Isolation Micro Kit, Thermo Fisher Scientific). The concentration and purity of the RNA samples were determined using an ND-1000 spectrophotometer (Thermo Fisher Scientific, Waltham, MA). Only samples with a 260/280 ratio between 1.9 and 2.1 were considered for analysis. The RNA samples were stored at −80 °C indefinitely.

Following purification of RNA, cDNA was synthesized using a Tetro cDNA Synthesis Kit (Bioline, London, UK) according to the manufacturer's protocol. A 20 µl reaction mixture was used in conjunction with 1 µg RNA, 500 ng oligo(dT) primer, and 200 U reverse transcriptase. Gene expression was measured via qRT-PCT using TaqMan hydrolysis probes (Thermo Fisher Scientific), as shown in Table 2. The TaqMan probes, cDNA, and TaqMan Gene Expression Master Mix (Thermo Fisher Scientific) were plated in a 384-well transparent plate, and amplification of each sample was performed in technical duplicate using a QuantStudio 12 K Flex real-time polymerase chain reaction (RT-PCR) machine (Thermo Fisher Scientific). Analysis was performed using the comparative cycle threshold method (ΔΔCt). The relative fold change was expressed as a percentage change compared to negative siRNA or PBS controls and normalized to two reference genes, *Actβ* and *Hprt1* for when *Gapdh* was assayed in knockdown experiments, and *Gapdh* and *Actβ* for all others.

Statistics: All graphing and statistical analysis was performed using Prism 6 (GraphPad Software, San Diego, CA). Statistically significant trends in time-course data sets were ascertained using a one-way or two-way ANOVA to determine statistical significance ($p<0.05$); Tukey's or Sidak's post hoc tests were applied where multiple statistical comparisons were required. An unpaired Student's *t* test was used for single comparisons.

RESULTS

Inflammatory and cell death profile at 24 h post-Invivofectamine 3.0 injection: Two previous formulations of Invivofectamine (Invivofectamine 1MFG and Invivofectamine 2.0) displayed a change in the inflammatory profile of the retina following delivery (Appendix 1). This presented with IBA1 positive cells exhibiting an amoeboid, activated profile and moving toward the GCL and vitreous body, which is where the formulation was injected. This observation indicates recruitment of resting mononuclear phagocytes (microglia and macrophages) to an inflammatory site. Quantification of this revealed a statistically significant difference in the IBA1 cell location in Invivofectamine 2.0-injected retinas (Appendix 1, $p>0.05$). The inflammatory profile following Invivofectamine 3.0 delivery required further evaluation. IBA1 positive mononuclear phagocytes displaying a resting, ramified morphology were evident in the control and Invivofectamine 3.0-injected eyes (Figure 3A–D). Mononuclear phagocytes appeared to have a normal distribution within the GCL, inner plexiform layer (IPL), and INL of the retinal tissue in the untreated needle-stick and PBS controls, as well as in the Invivofectamine 3.0-injected retinas. Using a general stress marker (GFAP), no differences were shown in the expression profile between the needle-stick and PBS controls when compared with Invivofectamine 3.0 (Figure 3E–H). The TUNEL assay showed that there was no discernible difference in TUNEL positive photoreceptor cells in the ONL of the Invivofectamine 3.0-injected and control animals (Figure 3I–L). Quantification of the total number of IBA1 labeled cells in each retinal section revealed no difference between any of the control animals and the Invivofectamine 3.0-injected animals (Figure 3M, $p>0.05$).

A suite of retinal stress and inflammatory primers was run using quantitative real time polymerase chain reaction (qRT-PCR) to further investigate the retinal profile after Invivofectamine 3.0 injection. There were no statistically significant changes in the expression of the stress and inflammatory markers tested (*Il-1β, Nox3, Fgf-2, Ccl4, Ccl17, Cxcl11, Edn2, Socs1,* and *Stat6*) after 24 h post-injection with Invivofectamine 3.0 (Figure 3O, p>0.05). *Ccl2*, *Il-10*, and *Il-6* levels were undetermined (UD) as they were deemed too low for the software to effectively quantify.

Clinical safety indicators post-injection: After 24 h post-injection with Invivofectamine 3.0, OCT retinal (Figure 4A, C) and fundus images (Figure 4B, D) displayed no indication of retinal damage. There were no differences in the ONL thickness ratios taken from the superior region at 1 mm from the optic nerve (region of focal retinal damage in PD mice [32]), quantified from the OCT retinal images, compared with control animals injected with PBS (Figure 4E, p>0.05). The ERG cone a-wave and b-wave responses displayed no statistically significant differences between the Invivofectamine 3.0-injected animals and the PBS control animals (Figure 4F–H, p>0.05).

After 7 days post-injection, there was no difference in the ONL thickness ratios, again quantified from the OCT retinal

Table 2. TaqMan hydrolysis probes for quantitative real-time PCR.

Gene	Entrez gene ID	Catalogue number
Actβ **(Actin-β)**	81,822 11,467	Rn00667869_m1 Mm01205647_g1
C3 **(Complement component c3)**	12,266	Mm00437858-m1
Ccl2 **(Chemokine (C-C motif) ligand 2)**	24,770	Rn01456716_g1
Ccl4 **(Chemokine (C-C motif) ligand 4)**	116,637	Rn00671924_m1
Ccl17 **(Chemokine (C-C motif) ligand 17)**	117,518	Rn01536936_g1
Cxcl11 **(Chemokine (C-X-C motif) ligand 11)**	305,236	Rn00788261_g1
Edn2 **(Endothelin 2)**	24,324	Rn00561135_m1
Fgf2 **(Fibroblast growth factor 2)**	54,250	Rn00570809_m1
Gapdh **(Glyceraldehyde-3-phosphate dehydrogenase)**	24,383 14,433	Rn99999916_s1 Mm01536933_m1
Hprt1 **(Hypoxanthine-guanine phosphoribosyl-transferase 1)**	24,465	Rn01527840_m1
Il-1β **(Interleukin 1β)**	24,494	Rn00580432_m1
Il-6 **(Interleukin 6)**	24,498	Rn01410330_m1
Il-10 **(Interleukin 10)**	25,325	Rn01483988_g1
Nox3 **(NADPH oxidase 3)**	292,279	Rn01430441_m1
Socs1 **(Suppressor of cytokine signaling 1)**	252,971	Rn00595838_s1
Stat6 **(Signal transducer and activator of transducin 6)**	362,896	Rn01505881_m1

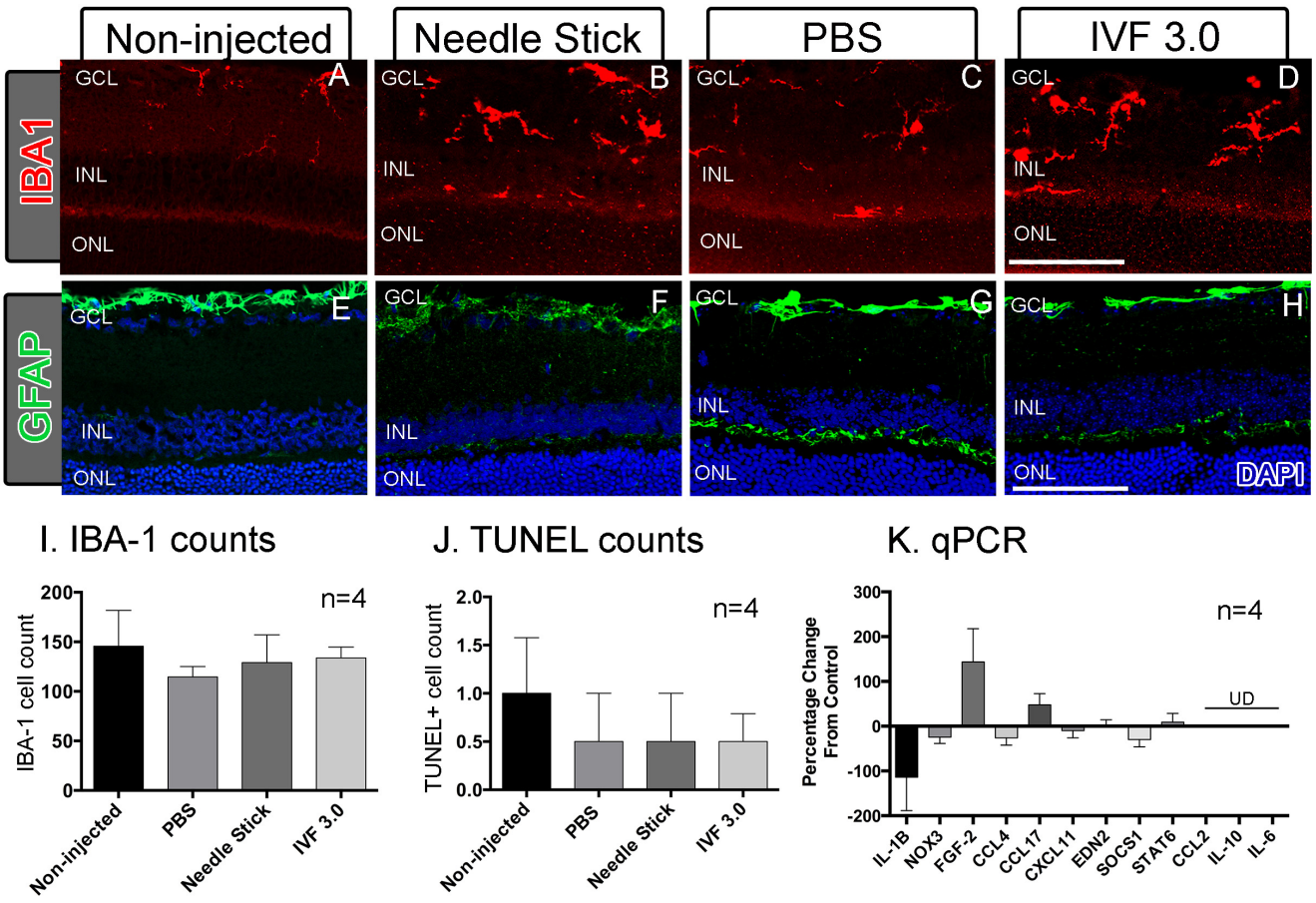

Figure 3. Histological indicators of cellular stress in the retina 24 h post-injection. **A**-**D**: IBA1-positive microglia (labelled in red) had a normal ramified shape and distribution profile within the inner layers of the retina. This was true for non-injected, PBS and needle stick controls as well as IVF injected animals. **E**-**H**: GFAP labelling had similar distribution profiles in controls and in treatment conditions, with a horizontal labelling pattern present only at the inner limiting membrane (ILM) and beneath the inner nuclear layer (INL), with no evidence of radial / vertical Müller cell process labelling. **I**: Quantification of IBA-1 positive cells revealed no differences between samples. **J**: Quantification of TUNEL-positive cells (labelling not shown) also showed no changes in the rates of cell death between samples. **K**: Quantitative real-time polymerase chain reaction (qRT-PCR) showed no significant changes in expression for a suite of inflammatory and retinal stress genes in IVF 3.0 injected animals compared to PBS injected controls. *Ccl2, Il-10* and *Il-6* expression were undetermined (UD, expression levels were too low for the software to detect; n=4, scale bars represent 100 µm).

images, between the Invivofectamine 3.0-injected and PBS control animals (Figure 4I, p>0.05). The same was seen with the 7-day post-injection ERG responses, with the cone a-wave and b-wave responses all showing no changes (Figure 4J–L, p>0.05), indicating no difference in ERG response between these treatment groups.

Gene knockdown efficiency: We also compared the efficacy of Invivofectamine 3.0 with another commercially available lipid-based transfection reagent, *in vivo*-jetPEI® (Polyplus transfection), demonstrating that Invivofectamine 3.0 had a greater knockdown capability at the earliest time point as *Gapdh* siRNA encapsulated at *in vivo*-jetPEI® displayed no statistically significant difference from the control (Figure 5A, p<0.05). However, the *in vivo*-jetPEI® could deliver the siRNA only at a maximum concentration of 0.5 µg/µl as opposed to the 1 µg/µl allowed for Invivofectamine 3.0. To test the duration of the targeted gene knockdown following the intravitreal delivery of *Gapdh* siRNA, we analyzed retinal gene expression at 1, 3, 5, and 7 days post-injection. A knockdown of *Gapdh*, when carried by Invivofectamine 3.0, was evident for up to 3 days post-injection, with 5 and 7 days post-injection showing no statistically significant knockdown compared to the PBS-injected controls (Figure 5B, p<0.05).

SiRNAs for *Il-1β* and *C3*, two major contributors to inflammation in the retina [37,38], were used to further test gene knockdown under stressed conditions induced by PD.

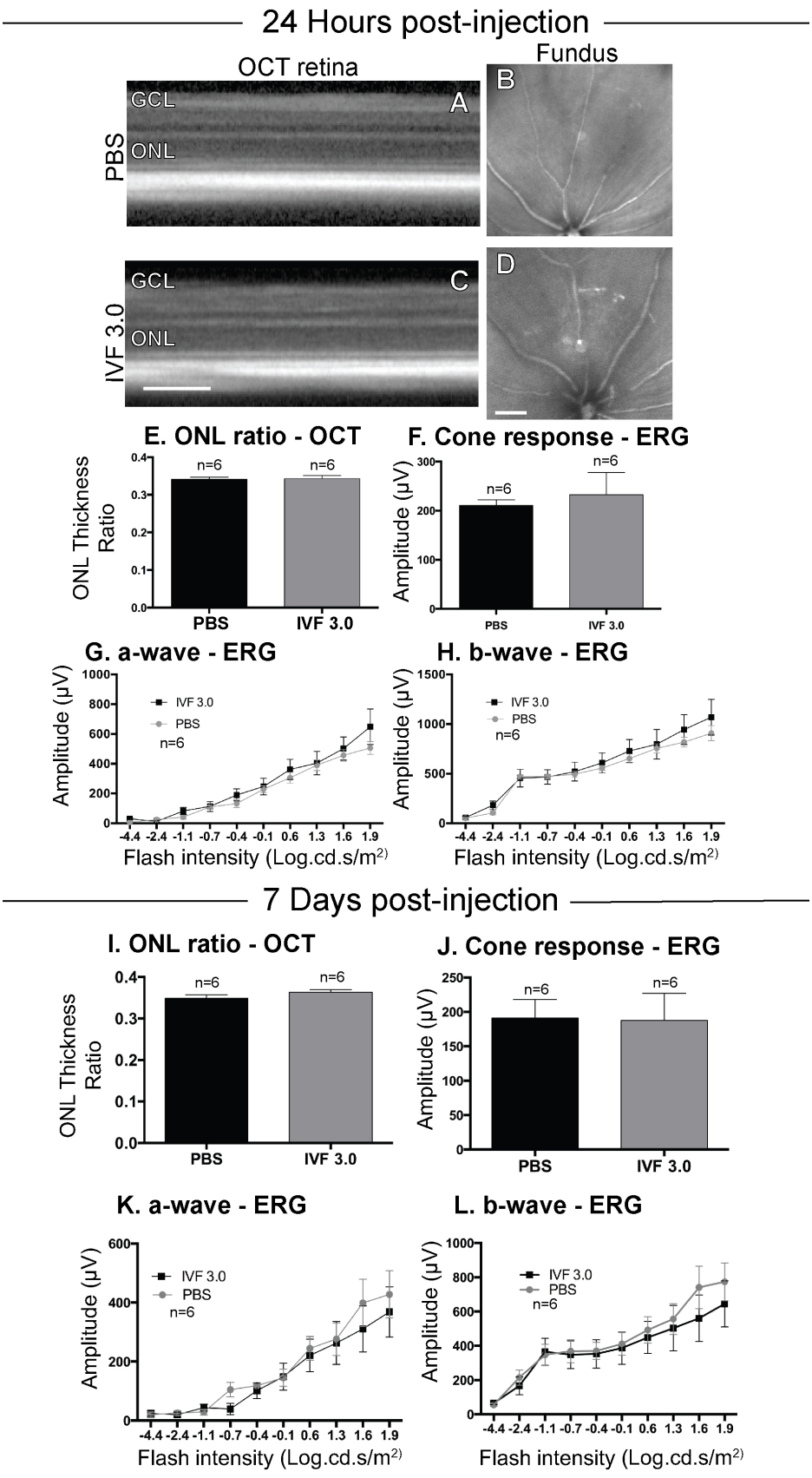

Figure 4. ERG and OCT indicating retinal safety and health following Invivofectamine 3.0 injection. **A**–**D**: Representative images of retinal and fundus images taken from the PBS control animals and the Invivofectamine 3.0-injected animals showed no indicators of retinal stress at 24 h post-injection. **E**: Outer nuclear layer (ONL) ratios measured at 24 h post-injection revealed no statistically significant differences between the PBS-injected controls and the Invivofectamine 3.0-injected animals. **F**–**H**: Cone a-wave and b-wave responses measured from electroretinography (ERG) showed no differences between the PBS-injected controls and the Invivofectamine 3.0-injected animals at 24 h post-injection. **I**: At 7 days post-injection, no differences were still seen in the ONL ratios between the two groups. **J**–**L**: Cone, a-wave and b-wave ERG responses again showed no differences at 7 days post-injection between the PBS-injected controls and the Invivofectamine 3.0-injected animals (*p<0.05 using unpaired Student *t* test (**E**, **F**, **I**, **J**) and two-way ANOVA with Sidak's post hoc test (**G**, **H**, **K**, **L**), n=6, scale bar represents 200 µm).

Il-1β siRNA injection with Invivofectamine 3.0 showed a statistically significant knockdown of *Il-1β* by approximately 900% at 48 h post-injection when compared to the negative siRNA controls (Figure 5B, p<0.05). Injection with *C3* siRNA encapsulated with Invivofectamine 3.0 also resulted in statistically significant knockdown of *C3* for 4 days post-injection when compared to the animals injected with negative siRNA controls following PD (Figure 5C, p<0.05).

Retinal location of Invivofectamine 3.0 delivery: We used Invivofectamine 3.0 in combination with Block-It siRNA (Thermo Fisher Scientific) to visualize the localization of Invivofectamine 3.0 delivery of fluorescent siRNA within the retina. The negative control showed low levels of fluorescence with only background autofluorescent staining visible in the outer segments (Figure 6A, B). An intravitreal injection with fluorescent Block-It led to fluorescence dispersed throughout all layers of the retina with the strongest amounts of fluorescent staining visualized in the central retina from the stitched whole retinal images (Figure 6C). Strong fluorescent staining could be seen throughout the GCL, INL, and ONL. In some instances, whole ganglion cells, bipolar cells,

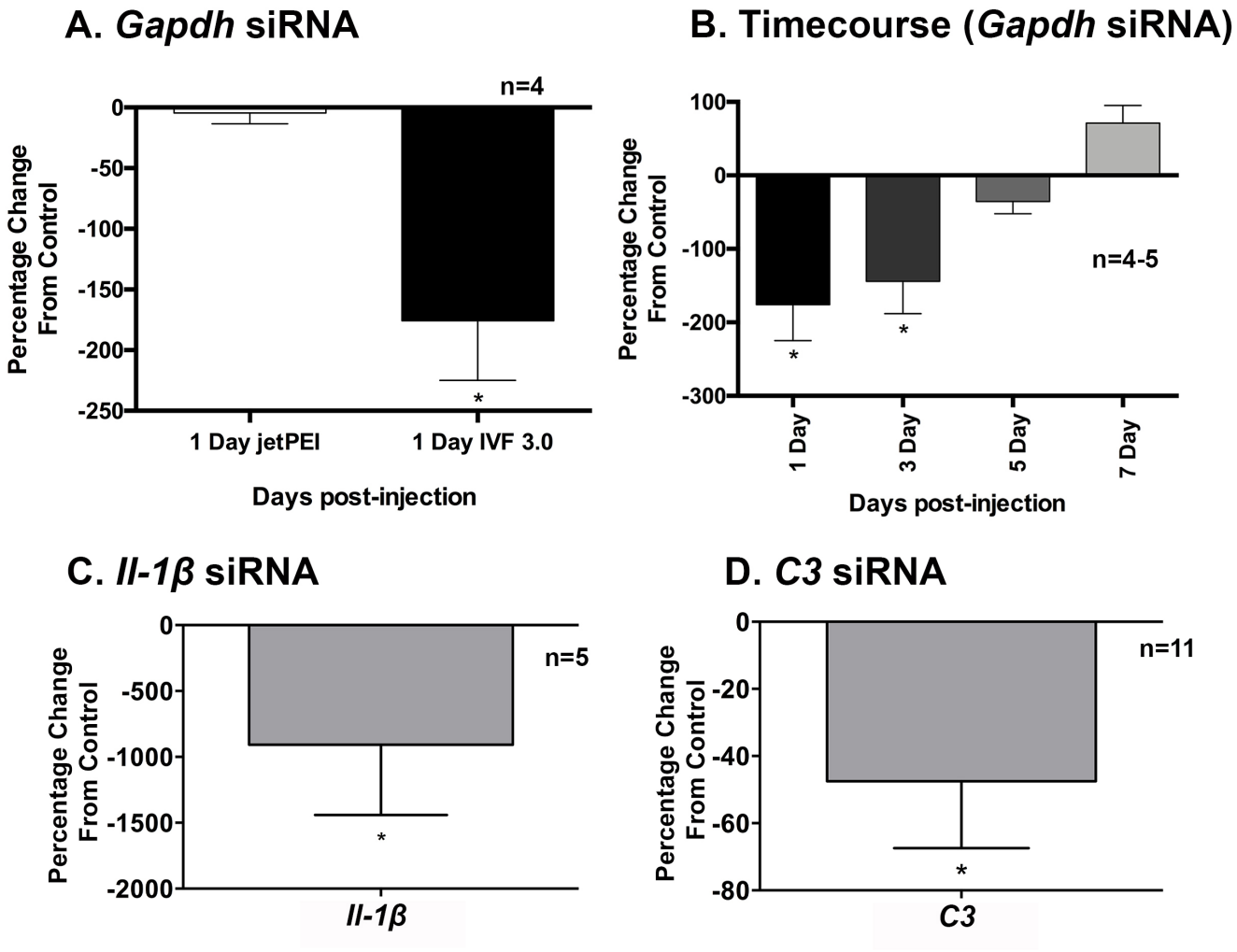

Figure 5. Efficiency of gene knockdown with Invivofectamine 3.0. **A**: *In vivo*-jetPEI®:*Gapdh* siRNA produced no statistically significant change in gene *Gapdh* expression 1 day post-injection when compared to controls whereas Invivofectamine 3.0 showed a statistically significant knockdown. **B**: Invivofectamine 3.0:*Gapdh* siRNA produced statistically significant targeted gene knockdown of *Gapdh* at 1 and 3 days post-injection. Five and 7 days showed no statistically significant difference compared to negative siRNA controls. **C**: Invivofectamine 3.0 complexed with siRNA against the inflammatory chemokine *Il-1β* also produced statistically significant knockdown. **D**: Invivofectamine 3.0:*C3* siRNA allowed for a statistically significant gene knockdown as well (*p<0.05 using one-way ANOVA with Tukey's post hoc test (**A**) and unpaired Student *t* test (**C**, **D**), n=4–11).

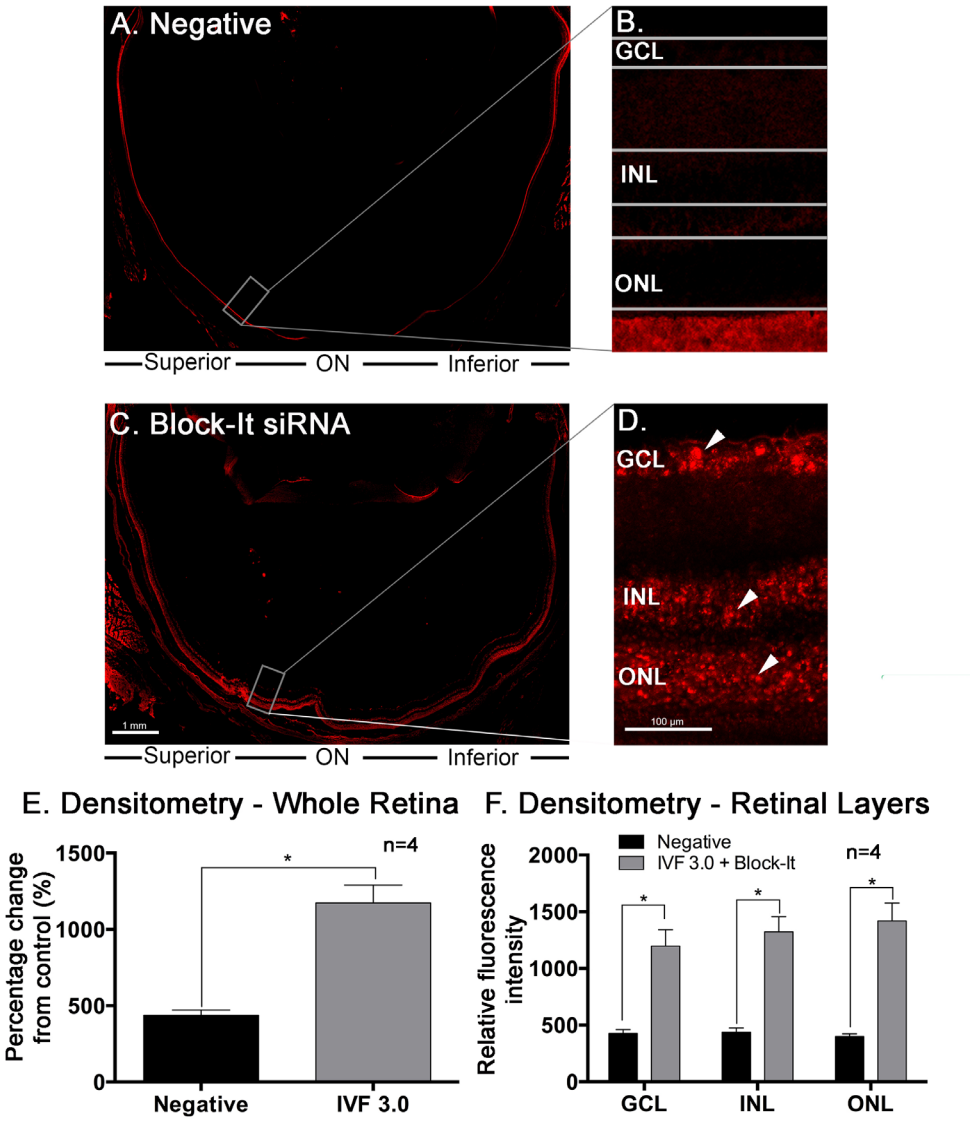

Figure 6. Localization of Invivofectamine 3.0 transfection with Block-It siRNA. **A**: Whole, stitched images of the retina show a representation of the distribution of Block-It siRNA with only autofluorescence of the outer segments in the negative control animals. **B**: Central images of the retina revealed no fluorescence in the negative siRNA-injected animals except autofluorescence of the outer segments. Grey lines indicate the cellular layers. **C**: Animals injected with Block-It display a similar pattern of autofluorescence but also have fluorescence visible in the inner and outer layers of the retina both peripherally and centrally. **D**: In the central retinal images, fluorescence can be seen throughout the ganglion cell layer (GCL), inner nuclear layer (INL), and outer nuclear layer (ONL) of the retina. Whole cells being transfected can be seen throughout the sections (white arrowheads). **E**: Quantification of fluorescence intensity revealed a statistically significant increase in animals injected with Block-It siRNA when compared to those injected with negative siRNA. **F**: Densitometry measurements of the retinal layers revealed statistically significant increases in fluorescence in the GCL, INL, and ONL in animals injected with Block-It (*p<0.05 using unpaired Student *t* test, n=4).

and photoreceptors were transfected (Figure 6D, indicated by the arrows).

Quantitative analysis of the fluorescence seen post-injection revealed a statistically significant increase in the fluorescence intensity of the Block-It siRNA when compared to negative siRNA-injected retinas when measuring all retinal layers from the OLM to the ILM (Figure 6E, $p<0.05$). The GCL, INL, and ONL all individually showed statistically significant increases in fluorescent staining in animals injected with Block-It siRNA when compared to negative controls (Figure 6F, $p<0.05$).

DISCUSSION

Delivery of nucleic acids into the retina will enable a greater understanding of the mechanisms behind normal retinal function, paving the way for novel therapeutics and treatment strategies, not only for retinal disorders but also other neurodegenerative diseases. In this study, we demonstrated that the intravitreal delivery of Invivofectamine 3.0 provides a reliable and safe transfection method of siRNA into all layers of the retina. First, we found that injection with Invivofectamine 3.0 results in no signs of increased immunogenicity, general stress, or cell death. Second, we found no statistically significant changes in retinal function or morphology after intravitreal administration of Invivofectamine 3.0 up to 1 week post-injection. Third, we found that Invivofectamine 3.0 penetrates the inner retina and the outer retina, providing up to 3–4 days of statistically significant, targeted gene knockdown from a single injection. Taken together, we demonstrated the use of Invivofectamine 3.0 is a quick and efficient method for studying the effects of nucleic acid delivery globally in the retina.

One of the primary issues with gene delivery vehicles is the ability for transfection into the relevant cell type, let alone the retina itself [39]. Non-viral and viral systems have had trouble with efficient penetration into the inner and outer retinal layers in vivo. The method of gene vector delivery into the eye plays a role in this, due to the many layers of the retina and the differing efficiencies of transfection into those layers. The two primary injection techniques for retinal transfection are subretinal and intravitreal injections. Although subretinal injections are efficient in transfecting the two cell types (photoreceptors and RPE) that contribute to many retinal degenerations, they are technically challenging and invasive by nature, with evidence of foveal thinning, macular holes, choroidal effusions, and ocular hypo- and hypertension [40-42].

Intravitreal injection for gene vector administration, however, is less invasive as it allows for the broad distribution of vectors throughout the retina. Adverse effects associated with intravitreal injections are perceived to be short-term, with retinal detachment, endophthalmitis, and vitreous hemorrhaging all noted as possible complications [11,12,14]. Using the proposed method, Invivofectamine 3.0 can transfect the GCL, INL, and ONL of the retina through intravitreal injections, with all three layers showing significant transfection of siRNA when carried by Invivofectamine 3.0. There was evidence of whole cells being transfected in these three layers, with cells in all of these layers being clearly labeled. The fluorescence depicted in the figure had dissipated within 24 h, at which point visualization and imaging of the fluorescence were no longer possible. This could be due to leaching of the fluorescent tag. Increasing the nucleic acid dose is an immediate way in which the longevity may be maximized. Additionally, the size of the eye must be taken into account due to the volume of vitreous humor for intravitreal injections. Concentrations must be adjusted accordingly, and we found that successful transfection in the mouse eye requires a larger relative nucleic concentration for its size. However, we are confident with the gene expression knockdown results of up to 3–4 days, and therefore, the quick half-life of the fluorescent tag in the retina was not a major concern.

Successful gene therapies require safe and effective delivery systems, with minimal side effects. When comparing the two broad classes of delivery systems currently available (viral and non-viral), non-viral systems appear to be more easily produced, less toxic, and less immunogenic [23,24,43,44]. In this study, we showed that Invivofectamine 3.0 has low levels of immunogenicity or acute toxicity in the retina, allowing for the potential of repeated administration, which is limited using viral vectors [43]. Furthermore, using two clinical methods of analysis, we demonstrated no loss of retinal function using ERG, while OCT showed normal morphology, following Invivofectamine 3.0 transfection.

One of the reported major drawbacks of non-viral, lipid-based delivery systems is that they are reported to be less effective than their viral counterparts, rarely accomplishing transgene expression at therapeutic levels [39,45]. Various approaches have been used to improve this efficiency, including the use of nanocarriers [11,14]. In the present study, we showed that Invivofectamine 3.0 can sustain targeted gene knockdown for up to 3–4 days using an siRNA for *Gapdh*, which is abundant in the retina. Additionally, with siRNAs for *C3* and *Il-1β*, we demonstrated effective reduction of gene expression. *C3* and *Il-1β* are key mediators of inflammation in retinal degeneration with peak *C3* expression at 5–7 days of PD in mice [28,32] and peak *Il-1β* expression at 24 h of PD in rats [28]. In comparison with another commercially available lipid-based formulation, *in vivo*-jetPEI, only 0.5 µg/µl of siRNA could be encapsulated in a microinjection of 1 µl which is required for mouse eyes. This does not imply that siRNA at 1 µg/µl used with *in vivo*-jetPEI® would not perform in the same manner; however, with limitations in the current formulation, this concentration is not possible. This demonstrates the packaging capability of Invivofectamine 3.0, and the maximum siRNA allowed for in the Invivofectamine 3.0 preparation demonstrated statistically significant gene knockdown capabilities when compared with *in vivo*-jetPEI®.

The 3–4 day timeframe (*Gapdh*) may limit the suitability of Invivofectamine 3.0 for long-term use, but for future considerations, new strategies are needed to increase the efficacy of gene knockdown and the longevity of delivery, both key aspects of therapeutic gene delivery. To increase knockdown time, heavier modification of the nucleic acids themselves could be beneficial. For the formulation, increasing the proportion of pegylated lipids results in a longer retention time in the blood, but it has not been tested in an ocular model, and may result in a loss of efficacy. Although currently not as effective long-term as viral-based approaches, lipid-based transfection is useful for proof-of-principle studies, and has been demonstrated to be effective in models of focal retinal degeneration [28,46,47]. Additionally, with the advent of lipid-based topical vehicles that can reach the posterior part of the eye, such as myriocin [13], the ease with which we can study gene silencing effects in the retina may be even more improved in the near future.

Although we demonstrated successful transfection of the siRNA:Invivofectamine 3.0 complex through to the inner retina, an important distinction is that this approach does not provide for targeting of a particular retinal cell type leading to potential pan-retinal knockdown involving multiple cell types. Viral vectors can be adapted to target uptake by a specified cell type [48-50]. Similar approaches could be harnessed for non-viral vectors through the intrinsic design of the chemical vectors [39,51]. A previous study showed successful targeted delivery of DNA and siRNA tumor cells due to chemical modifications of the lipid-based delivery agent to contain specific antibodies that mediate this recognition [52]. To our knowledge, this has yet to be achieved in the retina.

The results of this study indicated that Invivofectamine 3.0 is an effective tool for expediting gene function studies and identifying possible therapeutics in the neural retina. We demonstrated that a single injection of this lipid-based transfection of siRNA was able to penetrate all layers of the rodent retina and allowed for up to 3–4 days of targeted gene knockdown. If the longevity of the gene knockdown can be increased further, lipid-based transfection may be considered a time-effective alternative to viral-based strategies for ocular gene expression studies.

APPENDIX 1. INFLAMMATORY PROFILE OF INVIVOFECTAMINE FORMULATIONS.

To access the data, click or select the words "Appendix 1." (A-J) The IBA1 profile following the delivery of various Invivofectamine formulations was visualized with an increase in amoeboid, activated microglia present in Invivofectamine 1M and 2.0 formulations. (K) Quantification determined an increase in IBA1 positive microglia in Invivofectamine 2.0 in the ganglion cell layer of the retina. (L) No differences in TUNEL were observed (*p<0.05, one-way ANOVA with Tukey's post hoc test).

ACKNOWLEDGMENTS

This study was partly supported through funding from the Thermo Fisher Scientific Applications and Claims Expansions Grant with two of the authors (NA and XM) members of the Thermo Fisher Scientific team. Other funding bodies are The National Health and Medical Research Council (APP1127705, 2017-2019), the Australian Government Research Training Program Scholarship and the Australian National University Translational Fellowship. The authors do not have any other competing interests or conflicts of interest to disclose with regards to this paper.

REFERENCES

1. Ali RR, Sarra GM, Stephens C, Alwis MD, Bainbridge JW, Munro PM, Fauser S, Reichel MB, Kinnon C, Hunt DM, Bhattacharya SS, Thrasher AJ. Restoration of photoreceptor ultrastructure and function in retinal degeneration slow mice by gene therapy. Nat Genet 2000; 25:306-10. [PMID: 10888879].

2. Besch D, Zrenner E. Prevention and therapy in hereditary retinal degenerations. Doc Ophthalmol 2003; 106:31-5. [PMID: 12675483].

3. Campochiaro PA. Potential applications for RNAi to probe pathogenesis and develop new treatments for ocular disorders. Gene Ther 2006; 13:559-62. [PMID: 16195702].

4. Kjellstrom S, Bush RA, Zeng Y, Takada Y, Sieving PA. Retinoschisin gene therapy and natural history in the Rs1h-KO mouse: long-term rescue from retinal degeneration. Invest Ophthalmol Vis Sci 2007; 48:3837-45. [PMID: 17652759].

5. Schlichtenbrede FC, da Cruz L, Stephens C, Smith AJ, Georgiadis A, Thrasher AJ, Bainbridge JW, Seeliger MW, Ali RR. Long-term evaluation of retinal function in Prph2Rd2/Rd2 mice following AAV-mediated gene replacement therapy. J Gene Med 2003; 5:757-64. [PMID: 12950066].

6. Gulyaeva LF, Kushlinskiy NE. Regulatory mechanisms of microRNA expression. J Transl Med 2016; 14:143-[PMID: 27197967].

7. Berber P, Grassmann F, Kiel C, Weber BH. An Eye on Age-Related Macular Degeneration: The Role of MicroRNAs in Disease Pathology. Mol Diagn Ther 2017; 21:31-43. [PMID: 27658786].

8. Li Z, Rana TM. Therapeutic targeting of microRNAs: current status and future challenges. Nat Rev Drug Discov 2014; 13:622-38. [PMID: 25011539].

9. Conley SM, Cai X, Naash MI. Nonviral ocular gene therapy: assessment and future directions. Curr Opin Mol Ther 2008; 10:456-63. [PMID: 18830921].

10. Oliveira AV, Rosa da Costa AM, Silva GA. Non-viral strategies for ocular gene delivery. Mater Sci Eng C 2017; 77:1275-89. [PMID: 28532005].

11. Bucolo C, Drago F, Salomone S. Ocular drug delivery: a clue from nanotechnology. Front Pharmacol 2012; 3:188-[PMID: 23125835].

12. Wadhwa S, Paliwal R, Paliwal SR, Vyas SP. Nanocarriers in ocular drug delivery: an update review. Curr Pharm Des 2009; 15:2724-50. [PMID: 19689343].

13. Platania CBM, Dei Cas M, Cianciolo S, Fidilio A, Lazzara F, Paroni R, Pignatello R, Strettoi E, Ghidoni R, Drago F, Bucolo C. Novel ophthalmic formulation of myriocin: implications in retinitis pigmentosa. Drug Deliv 2019; 26:237-43. [PMID: 30883241].

14. Amadio M, Pascale A, Cupri S, Pignatello R, Osera C. V DA, AG DA, Leggio GM, Ruozi B, Govoni S, Drago F, Bucolo C. Nanosystems based on siRNA silencing HuR expression counteract diabetic retinopathy in rat. Pharmacol Res 2016; 111:713-20. [PMID: 27475885].

15. Miyazaki M, Obata Y, Abe K, Furusu A, Koji T, Tabata Y, Kohno S. Gene transfer using nonviral delivery systems. Perit Dial Int 2006; 26:633-40. .

16. Nishikawa M, Hashida M. Nonviral approaches satisfying various requirements for effective in vivo gene therapy. Biol Pharm Bull 2002; 25:275-83. [PMID: 11913519].

17. Boye SE, Boye SL, Lewin AS, Hauswirth WW. A comprehensive review of retinal gene therapy. Mol Ther 2013; 21:509-19. .

18. Carvalho LS, Vandenberghe LH. Promising and delivering gene therapies for vision loss. Vision Res 2015; 111:124-33. .

19. Trapani I, Puppo A, Auricchio A. Vector platforms for gene therapy of inherited retinopathies. Prog Retin Eye Res 2014; 43:108-28. [PMID: 25124745].

20. Navarro J, Risco R, Toschi M, Schattman G. Gene therapy and intracytoplasmatic sperm injection (ICSI) - a review. Placenta 2008; 29:193-9. .

21. Kafri T, Morgan D, Krahl T, Sarvetnick N, Sherman L, Verma I. Cellular immune response to adenoviral vector infected cells does not require de novo viral gene expression: implications for gene therapy. Proc Natl Acad Sci USA 1998; 95:11377-82. [PMID: 9736744].

22. Thomas CE, Birkett D, Anozie I, Castro MG, Lowenstein PR. Acute direct adenoviral vector cytotoxicity and chronic, but not acute, inflammatory responses correlate with decreased vector-mediated transgene expression in the brain. Mol Ther 2001; 3:36-46. .

23. Bessis N. GarciaCozar FJ, Boissier MC. Immune responses to gene therapy vectors: influence on vector function and effector mechanisms. Gene Ther 2004; 11:Suppl 1S10-7. [PMID: 15454952].

24. Thomas CE, Ehrhardt A, Kay MA. Progress and problems with the use of viral vectors for gene therapy. Nat Rev Genet 2003; 4:346-58. [PMID: 12728277].

25. Han IC, Burnight E, Ulferts MJ, Worthington KS, Russell SR, Sohn EH, Mullins RF, Stone E, Tucker BA, Wiley LA. Helper-Dependent Adenovirus Transduces the Human and Rat Retina but Elicits an Inflammatory Reaction When Delivered Subretinally in Rats. Hum Gene Ther 2019; [PMID: 31456426].

26. Koirala A, Conley SM, Naash MI. A review of therapeutic prospects of non-viral gene therapy in the retinal pigment epithelium. Biomaterials 2013; 34:7158-67. [PMID: 23796578].

27. Rutar M, Natoli R, Provis JM. Small interfering RNA-mediated suppression of Ccl2 in Muller cells attenuates microglial recruitment and photoreceptor death following retinal degeneration. J Neuroinflammation 2012; 9:221-[PMID: 22992301].

28. Natoli R, Fernando N, Jiao H, Racic T, Madigan M, Barnett NL, Chu-Tan JA, Valter K, Provis J, Rutar M. Retinal Macrophages Synthesize C3 and Activate Complement in AMD and in Models of Focal Retinal Degeneration. Invest Ophthalmol Vis Sci 2017; 58:2977-90. [PMID: 28605809].

29. Matsuda T, Cepko CL. Electroporation and RNA interference in the rodent retina in vivo and in vitro. Proc Natl Acad Sci USA 2004; 101:16-22. [PMID: 14603031].

30. Pitkanen L, Pelkonen J, Ruponen M, Ronkko S, Urtti A. Neural retina limits the nonviral gene transfer to retinal pigment epithelium in an in vitro bovine eye model. AAPS J 2004; 6:e25[PMID: 15760110].

31. Rutar M, Provis JM, Valter K. Brief exposure to damaging light causes focal recruitment of macrophages, and long-term destabilization of photoreceptors in the albino rat retina. Curr Eye Res 2010; 35:631-43. [PMID: 20597649].

32. Natoli R, Jiao H, Barnett NL, Fernando N, Valter K, Provis JM, Rutar M. A model of progressive photo-oxidative degeneration and inflammation in the pigmented C57BL/6J mouse retina. Exp Eye Res 2016; 147:114-27. [PMID: 27155143].

33. Rutar M, Natoli R, Kozulin P, Valter K, Gatenby P, Provis JM. Analysis of complement expression in light-induced retinal degeneration: synthesis and deposition of C3 by microglia/macrophages is associated with focal photoreceptor degeneration. Invest Ophthalmol Vis Sci 2011; 52:5347-58. [PMID: 21571681].

34. Fernando N, Natoli R, Valter K, Provis J, Rutar M. The broad-spectrum chemokine inhibitor NR58–3.14.3 modulates macrophage-mediated inflammation in the diseased retina. J Neuroinflammation 2016; 13:47-[PMID: 26911327].

35. Natoli R, Zhu Y, Valter K, Bisti S, Eells J, Stone J. Gene and noncoding RNA regulation underlying photoreceptor protection: microarray study of dietary antioxidant saffron and photobiomodulation in rat retina. Mol Vis 2010; 16:1801-22. [PMID: 20844572].

36. Rutar M, Natoli R, Chia RX, Valter K, Provis JM. Chemokine-mediated inflammation in the degenerating retina is coordinated by Muller cells, activated microglia, and retinal pigment epithelium. J Neuroinflammation 2015; 12:8-[PMID: 25595590].

37. Anderson DH, Radeke MJ, Gallo NB, Chapin EA, Johnson PT, Curletti CR, Hancox LS, Hu J, Ebright JN, Malek G, Hauser MA, Rickman CB, Bok D, Hageman GS, Johnson LV. The pivotal role of the complement system in aging and age-related macular degeneration: hypothesis re-visited. Prog Retin Eye Res 2010; 29:95-112. [PMID: 19961953].

38. Zhao M, Bai Y, Xie W, Shi X, Li F, Yang F, Sun Y, Huang L, Li X. Interleukin-1beta Level Is Increased in Vitreous of Patients with Neovascular Age-Related Macular Degeneration (nAMD) and Polypoidal Choroidal Vasculopathy (PCV). PLoS One 2015; 10:e0125150[PMID: 25978536].

39. Al-Dosari MS, Gao X. Nonviral gene delivery: principle, limitations, and recent progress. AAPS J 2009; 11:671-81. [PMID: 19834816].

40. Jacobson SG, Cideciyan AV, Ratnakaram R, Heon E, Schwartz SB, Roman AJ, Peden MC, Aleman TS, Boye SL, Sumaroka A, Conlon TJ, Calcedo R, Pang JJ, Erger KE, Olivares MB, Mullins CL, Swider M, Kaushal S, Feuer WJ, Iannaccone A, Fishman GA, Stone EM, Byrne BJ, Hauswirth WW. Gene therapy for leber congenital amaurosis caused by RPE65 mutations: safety and efficacy in 15 children and adults followed up to 3 years. Arch Ophthalmol 2012; 130:9-24. [PMID: 21911650].

41. Maguire AM, Simonelli F, Pierce EA, Pugh EN Jr, Mingozzi F, Bennicelli J, Banfi S, Marshall KA, Testa F, Surace EM, Rossi S, Lyubarsky A, Arruda VR, Konkle B, Stone E, Sun J, Jacobs J, Dell'Osso L, Hertle R, Ma JX, Redmond TM, Zhu X, Hauck B, Zelenaia O, Shindler KS, Maguire MG, Wright JF, Volpe NJ, McDonnell JW, Auricchio A, High KA, Bennett J. Safety and efficacy of gene transfer for Leber's congenital amaurosis. N Engl J Med 2008; 358:2240-8. [PMID: 18441370].

42. Bloquel C, Bourges JL, Touchard E, Berdugo M, BenEzra D, Behar-Cohen F. Non-viral ocular gene therapy: potential ocular therapeutic avenues. Adv Drug Deliv Rev 2006; 58:1224-42. [PMID: 17095114].

43. Witlox MA, Lamfers ML, Wuisman PI, Curiel DT, Siegal GP. Evolving gene therapy approaches for osteosarcoma using viral vectors Bone 2007; 40:797-812. review[PMID: 17189720].

44. Halbert CL, Miller AD, McNamara S, Emerson J, Gibson RL, Ramsey B, Aitken ML. Prevalence of neutralizing antibodies against adeno-associated virus (AAV) types 2, 5, and 6 in cystic fibrosis and normal populations: Implications for gene therapy using AAV vectors. Hum Gene Ther 2006; 17:440-7. [PMID: 16610931].

45. Dang JM, Leong KW. Natural polymers for gene delivery and tissue engineering. Adv Drug Deliv Rev 2006; 58:487-99. [PMID: 16762443].

46. Chu-Tan JA, Rutar M, Saxena K, Aggio-Bruce R, Essex RW, Valter K, Jiao H, Fernando N, Wooff Y, Madigan MC, Provis J, Natoli R. MicroRNA-124 Dysregulation is Associated With Retinal Inflammation and Photoreceptor Death in the Degenerating Retina. Invest Ophthalmol Vis Sci 2018; 59:4094-105. [PMID: 30098196].

47. Natoli R, Fernando N, Madigan M, Chu-Tan JA, Valter K, Provis J, Rutar M. Microglia-derived IL-1beta promotes chemokine expression by Muller cells and RPE in focal retinal degeneration. Mol Neurodegener 2017; 12:31-[PMID: 28438165].

48. Kotterman MA, Schaffer DV. Engineering adeno-associated viruses for clinical gene therapy. Nat Rev Genet 2014; 15:445-51. [PMID: 24840552].

49. Petrs-Silva H, Linden R. Advances in recombinant adeno-associated viral vectors for gene delivery. Curr Gene Ther 2013; 13:335-45. [PMID: 24060313].

50. Schon C, Biel M, Michalakis S. Retinal gene delivery by adeno-associated virus (AAV) vectors: Strategies and applications. Eur J Pharm Biopharm 2015; 95:343-52. .

51. Simcikova M, Prather KL, Prazeres DM, Monteiro GA. Towards effective non-viral gene delivery vector. Biotechnol Genet Eng Rev 2015; 31:82-107. [PMID: 27160661].

52. Xu L, Huang CC, Huang W, Tang WH, Rait A, Yin YZ, Cruz I, Xiang LM, Pirollo KF, Chang EH. Systemic tumor-targeted gene delivery by anti-transferrin receptor scFv-immunoliposomes. Mol Cancer Ther 2002; 1:337-46. [PMID: 12489850].